Supporting Information

Bulletin of the Chemical Society of Japan

Tethering Organic Disulfides to Layered Silicates: A Versatile Strategy for Photo-Controllable Dynamic Chemistry and Functionalization

Jonathon Tanks,* Takashi Hiroi, Kenji Tamura, and Kimiyoshi Naito

Electronic Supporting Information for *Bulletin of the Chemical Society of Japan*

Supporting Information for

Tethering Organic Disulfides to Layered Silicates: A Versatile Strategy for Photo-controllable Dynamic Chemistry and Functionalization

Jonathon Tanks,*[1] Takashi Hiroi,[2] Kenji Tamura,[3] and Kimiyoshi Naito[1,4]

[1]Research Center for Structural Materials, National Institute for Materials Science (NIMS)

[2]International Center for Young Scientists, National Institute for Materials Science (NIMS)

[3]Research Center for Functional Materials, National Institute for Materials Science (NIMS)

[4]Department of Aerospace Engineering, Tohoku University

Disulfide Intercalation

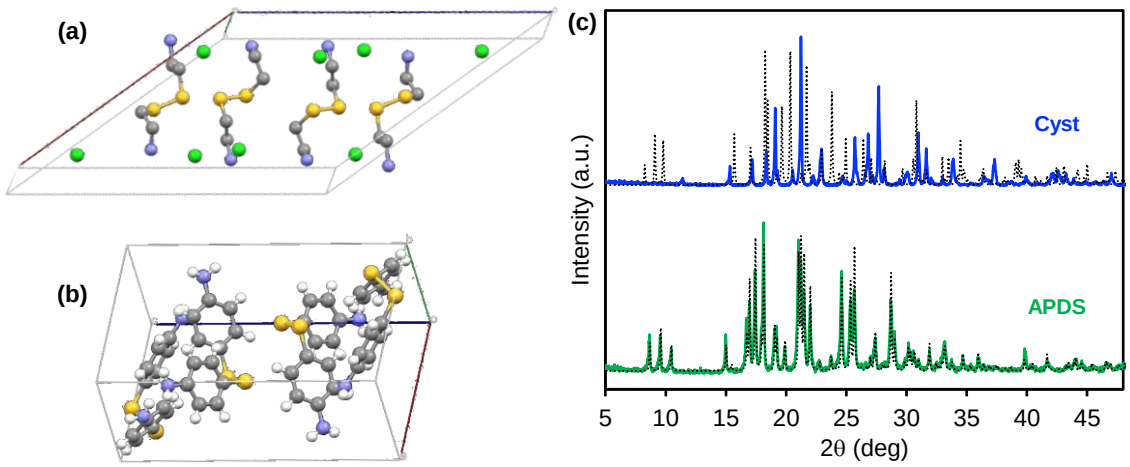

Figure S1. Crystal structures of *gauche* conformers (a) Cyst and (b) APDS; yellow = S, grey = C, blue = N, white = H, green = Cl. (c) Calculated diffraction patterns (black dotted lines) compared to experimental measurements. Significant deviation of Cyst patterns suggests the ideal *gauche* structure may not be dominant in the as-received powder.

In principle, the organo-modifier intercalates via electrostatic interactions with the negative layer charge in the silicate. The cation exchange capacity (CEC) of Na-TSM is about 120 meq/g, equating to 0.6 mmol/g of diamine-type intercalating agent. Disulfide contents of 0.58 mmol/g and 0.68 mmol/g were calculated from TGA for Cyst-TSM and APDS-TSM, respectively (Fig. S2a). FTIR spectra show appearance of the benzene (APDS) and ethylene (Cyst) peaks compared to Na-TSM, and the decreased -OH peak (3200-3600 cm^{-1}) confirms that the disulfides intercalate via cation exchange (Fig. S2b).

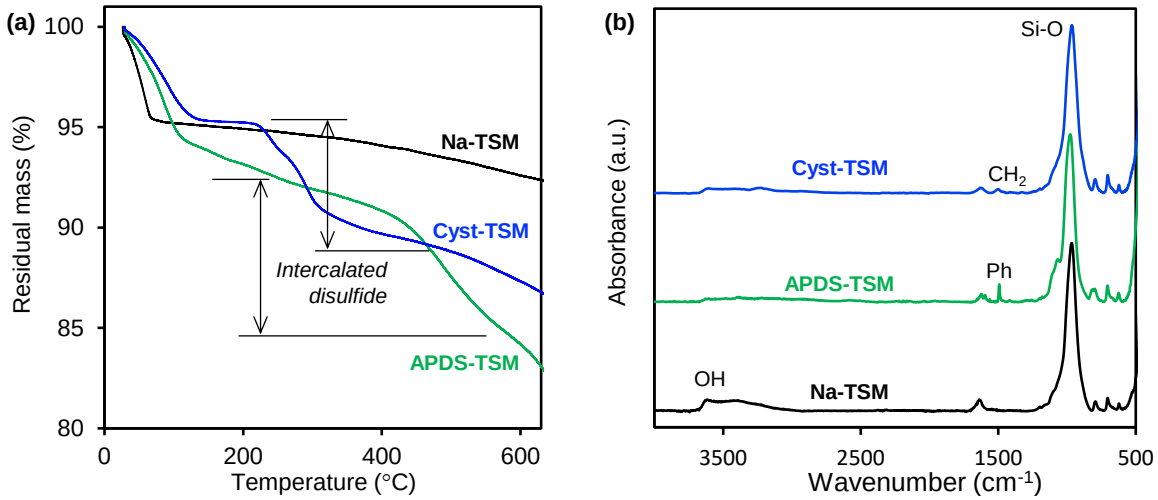

Figure S2. (a) TGA mass-loss curves and (b) ATR-FTIR spectra of disulfide-intercalated silicates.

Disulfide Exchange Reactions

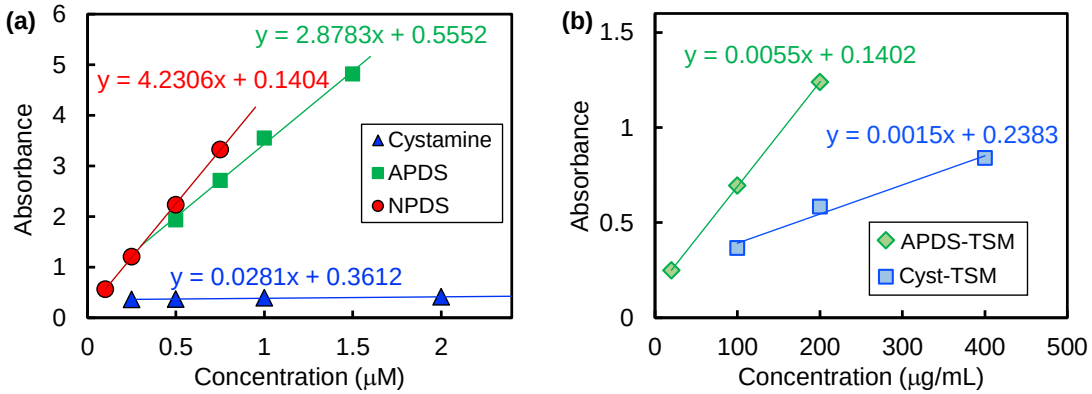

Figure S3. Calibration curves of (a) disulfide reagents and (b) intercalated silicates; peak absorbance taken at 311 nm (APDS), 322 nm (NPDS), and 281 nm (Cyst).

Our objective in the current study was not to efficiently exfoliate the layered silicates, but rather to investigate the disulfide-based reactions inside the interlayer. However, to emphasize the swelling effect of DMSO, we captured AFM images of APDS-TSM in DMSO and water (for comparison). No statistical data is available, but a cursory observation showed that particles in DMSO had smaller thickness, possibly between 4-10 layers (compared to 8-15). Furthermore, the nanosheets collected from dispersion in DMSO showed negligible change from the initial material, strongly indicating that neither APDS nor Cyst undergo permanent scission (e.g., reduction) in solvent. These functional nanosheets can be dispersed, recovered and reused for a variety of applications.

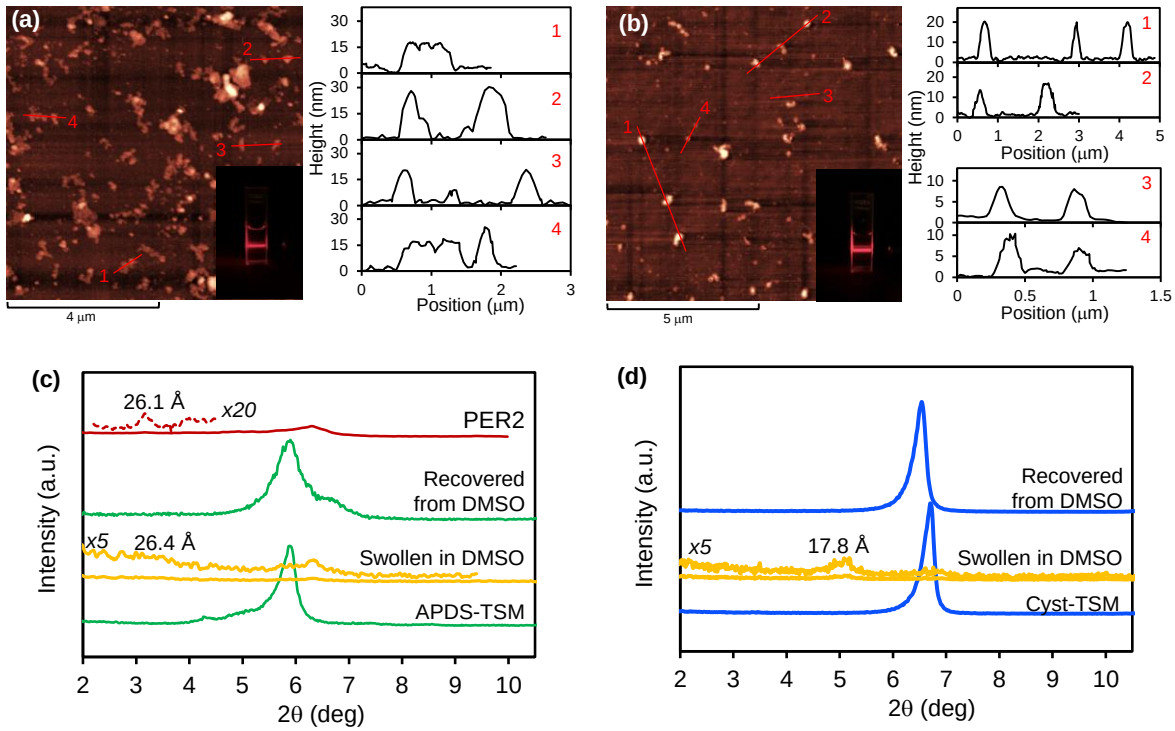

Figure S4. AFM height profiles and photos of the Tyndall effect for (a) water and (b) DMSO dispersions of APDS-TSM. While there were many large agglomerates in both solvents, DMSO showed smaller particle heights overall, suggesting more exfoliation than water. XRD patterns of (c) APDS-TSM and (d) Cyst-TSM before, during, and after swelling in DMSO.

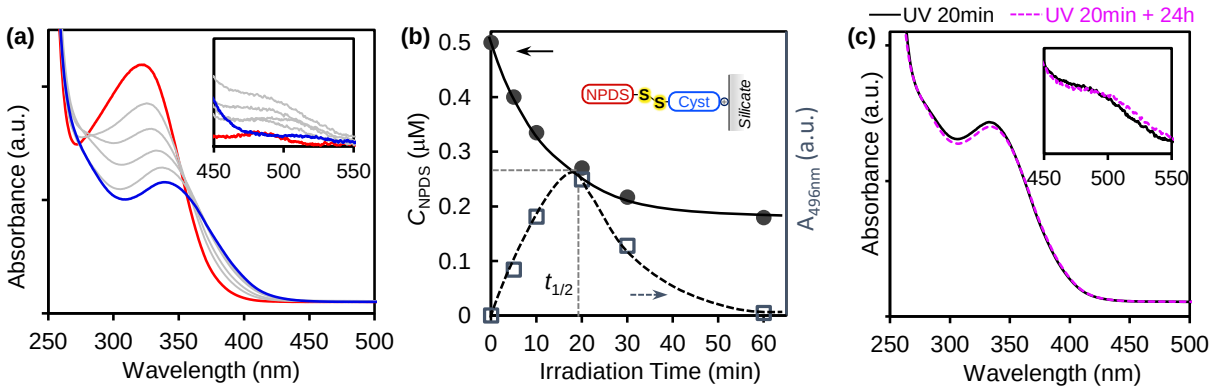

Figure S5. (a) UV-vis spectra of **PER3** reaction mixture, (b) change in NPDS concentration and reaction intermediate (496 nm) during irradiation in **PER3**, and (c) UV-vis spectra taken after 20 min of UV radiation and then again 24 h later.

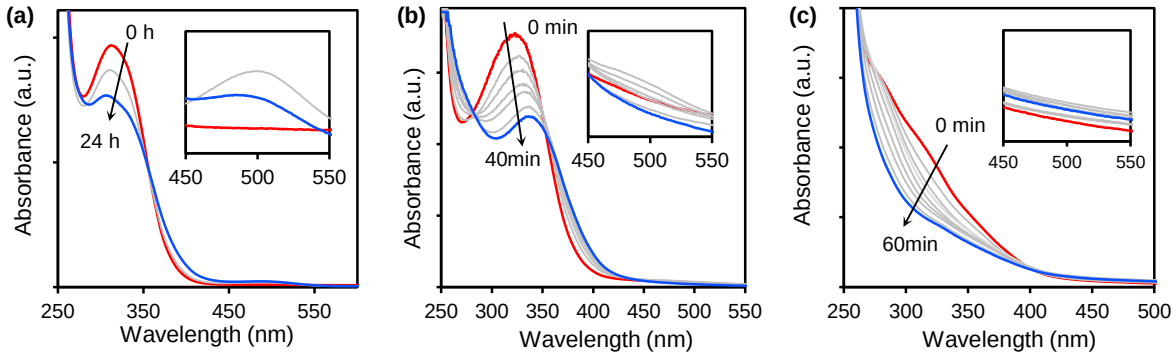

Figure S6. (a) "Indiscriminate" disulfide exchange between APDS/NPDS in DMSO and no UV light. (b) UV-vis spectra of **PER2′** using APDS-TSM that was recovered from DMSO, showing no significant change from the original disulfide-intercalated silicate. (c) UV-vis spectra of **PER4**, showing the apparent disulfide-thiol exchange between APDS-TSM and *β*-ME.

Disulfide-Initiated in-situ Polymerization

We stopped the curing when the films felt solid without tack, which tended to be around 15% conversion by FTIR. We expect a large quantity of unreacted monomer to be immobilized as the film cures. However, our objective was not to fabricate a "perfect" film with unique properties, but rather to simply demonstrate the versatility of disulfide-functionalized nanosheets.

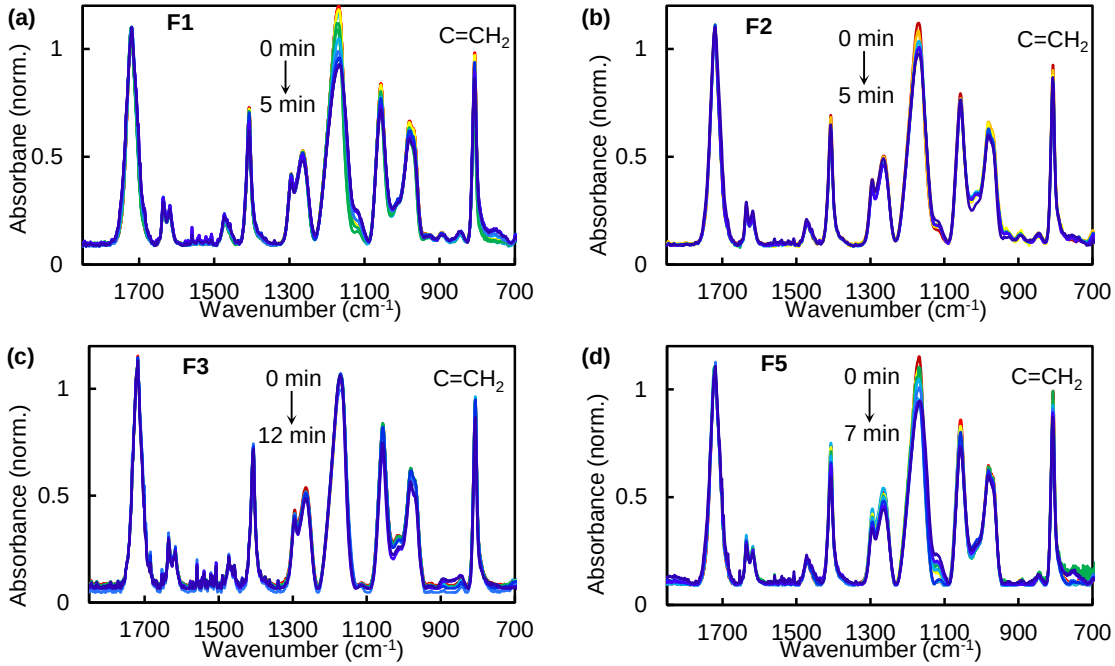

Figure S7. ATR-FTIR spectra of acrylate films (a) **F1**, (b) **F2**, (c) **F3**, and (d) **F5**. The conversion was calculated by the area under the peak at 807 cm^{-1} ($C=CH_2$).

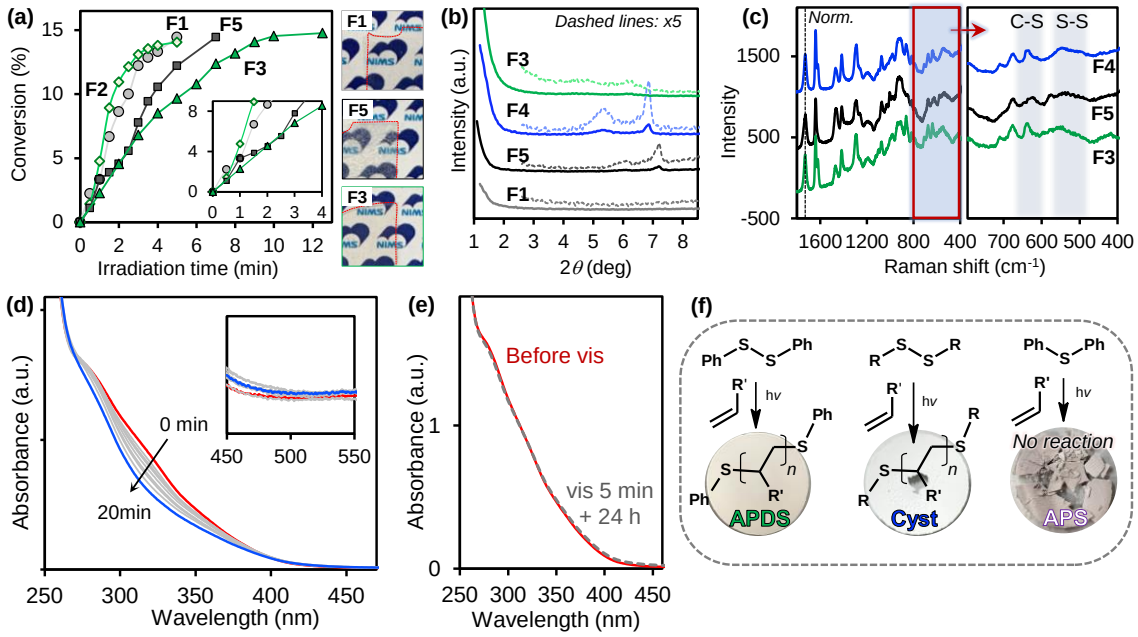

Figure S8. (a) Curing rates and (b) XRD patterns of films **F1-3** and **F5**, and (c) Raman spectra of films **F3-F5**. (d) UV-vis spectra of the **F3** mixture dispersed in DMSO and irradiated with UV, showing a decrease in the APDS peak with no intermediate. (e) The same mixture that was irradiated with visible light (490 nm cut-off filter) then left for 24 h showed no significant changes, indicating the thiyl radical-mediated *in-situ* polymerization can be controlled by wavelength. (f) PETA/TSM films fabricated by UV radiation and filtration, showing that S-S scission generates radicals for polymerization rather than C-S scission.